

France 1  
UK 1/1/1/1/1  
Can 1  
US 1  
Nash 1

5  
1  
1  
1

## Spatial integration characteristics in motion detection and direction identification\*

ANDREI GOREA

*Laboratoire de Psychologie Expérimentale, Université René Descartes et EPHE 3ème section, associé au CNRS, 28 rue Serpente, 75006 Paris, France*

Received 11 February 1985; in revised form 14 June 1985; accepted 17 June 1985

**Abstract**—Spatial integration characteristics were assessed with drifting gratings for both detection and direction-identification contrast thresholds. Thresholds were measured while stimulus width, length or both were varied. It was found that: (1) the shape of the size/sensitivity functions changes with spatial, but not with temporal, frequency; (2) direction-identification thresholds diverge from the detection thresholds below 1 cycle but can be reliably measured for stimulus widths as small as 0.1275 cycles; (3) the integration characteristics are slightly anisotropic for the identification but not for the detection process, and (4) the two-dimensional spatial integration cannot be directly predicted from its one-dimensional characteristics. Width/sensitivity detection functions are well fitted by predictions of Wilson and Bergen's four-channel model. Predictions from a temporal covariance model provide a poor fit to the identification data. It is argued that classes of detection and direction-identification models must involve identical nonlinearities prior to their respective thresholds. It is concluded that the hypothesis according to which both performances are determined by the same spatial integration stage cannot be rejected.

### INTRODUCTION

At the detection threshold, opposite directions of movement ( $180^\circ$  apart) are addressing independent movement detectors: evidence for this is based on the observation that the contrast threshold for a counterphase modulated grating is twice as high as the contrast threshold for a drifting stimulus with the same spatio-temporal characteristics (Levinson and Sekuler, 1975; Kelly, 1979). Since the counterphase stimulus is mathematically equivalent to the linear summation of two gratings drifting in opposite directions it can be inferred that the former is detected whenever one of its components attains its own detection threshold. Therefore the two components appear to be detected independently.<sup>1</sup> This is not true for the whole spatio-temporal domain. At high spatial and low temporal frequencies the contrast threshold for a counterphase stimulus is much less than twice the contrast threshold for one of its components (Stromeyer *et al.*, 1978; Kulikowski, 1978; Watson *et al.*, 1980; Gorea and Lorenceau, 1984). This has been taken as evidence for contrast summation at the detection threshold suggesting a lack of directional selectivity within this spatio-temporal range.

The independence of directionally selective mechanisms cannot be specified in terms of the velocity of the stimulus; when the sensitivity ratios between drifting and counterphase modulated gratings are plotted in the spatio-temporal plane, the 'isotropy' contours are typically circular rather than elongated along a given constant velocity (Gorea and Lorenceau, 1984).

\*Parts of this work were presented at the *VIIIth Conference on Visual Perception*, Cambridge, UK, 1984.

*Detection and identification of drifting gratings*

The existence of directionally selective mechanisms does not imply that the visual system is provided with specific, directional information. This would be so to the extent that the directional mechanisms were *labelled* such that any time they are activated, an unambiguous directional response would also be triggered (Watson and Robson, 1981).<sup>2</sup> Under this hypothesis, contrast thresholds for detection and identification of opposite directions of drift should be identical at least within that spatio-temporal range where they were shown to be detected independently. Although such evidence has been provided in electrophysiology (Kulikowski *et al.*, 1977) and psychophysics (Ball *et al.*, 1983), departures from this hypothesis have been reported also. Green (1983) and Pasternak and Merigan (1984) showed an inverse proportionality between velocity and direction-identification thresholds independently of the particular combinations of spatial and temporal frequencies. As mentioned above, direction independence as measured by the drift-to-counterphase threshold ratio does not depend on velocity.

These results point to the difficulty of specifying the nature of the relationship between *independent* and *labelled* detectors, or, in a more general sense, between detection and identification. Within this theoretical framework this study raises the problem of the distinction between mechanisms subserving the detection of a spatio-temporally modulated stimulus and mechanisms responsible for the identification of its direction of drift. One way to approach this problem is to determine the spatial integration characteristics of the processes underlying each of these two different tasks. The measure of the spatial integration characteristics can then be used to describe the space domain sensitivity weighting functions of the mechanisms involved and permits therefore their direct comparison. Following the same line of reasoning Gorea (1984) showed that time integration characteristics in spatial frequency detection and discrimination cannot be distinguished from one another.

*Psychophysical receptive fields*

The spatial integration characteristics of the visual system have been revealed by measuring either the area/sensitivity function, or the 'line spread function' (LSF—also called 'psychophysical receptive field' or 'element contribution function'). Under the reasonable assumption of linearity at threshold, the two approaches are complementary; linear analysis permits the prediction of the area/sensitivity function from the LSF and the reverse.

The area/sensitivity relationship was first mentioned by Aubert (1865) and generalized by Ricco (1877) for small stimulus sizes. As a general rule, subsequent investigations were concerned with the description of the relationship between luminance sensitivity and the size of spatially homogeneous test stimuli [see Bartlett (1965) for a review of this early literature]. The introduction of sinusoidal gratings in visual psychophysics (Shade, 1956) on the one hand, and the proposal of a general model of the visual system as a spatial frequency analyser (Campbell and Robson, 1968) on the other, led to the specification of the area integration characteristics in terms of the number of cycles of grating stimuli, rather than in terms of their absolute spatial extent (Hoekstra *et al.*, 1974; Savoy and McCann, 1975; McCann *et al.*, 1978; Howell and Hess, 1978; Jamar and Koenderink, 1983; van der Wildt and Waarts, 1983). Different interpretations of the area effects were provided depending on whether one or multiple channel models were adopted to account for the data (see Legge, 1978 for a review of

these problems). More recently, the introduction of the probability summation concept by Quick (1974) and Graham (1977) led to even more sophisticated (but also more efficient) models accounting for the spatial integration characteristics of the visual system (Legge, 1978; Robson and Graham, 1981).

The direct measurement of the 'element contribution function' was first reported by Westheimer (1965, 1967) who obtained differential thresholds for a central flashing spot as a function of the diameter of a circular masking background. Different techniques were subsequently used by Thomas (1968), Fiorentini (1971), Kulikowski and King-Smith (1973), King-Smith and Kulikowski (1975) and Hines (1976) to achieve similar results. Whether the best analytical expression to account for these measurements is a DOG function (difference of Gaussians—Wilson, 1978a, b), the Laplacian operator (Marr and Hildreth, 1980), or a Gabor function (Daugman, 1980; Marcelja, 1980; Watson, 1982), is of little practical interest since all these models provide similar predictions. What appears to be a much more critical parameter in fitting the measured LSFs is the application of probability summation across space and channels. Depending on whether this parameter is, or is not, taken into account, the same empirical results can be modeled as reflecting the probabilistically combined sensitivities of many independent channels (Wilson and Bergen, 1979; Bergen *et al.*, 1979), or the sensitivity profile of one single mechanism (e.g. Kulikowski and King-Smith, 1973; King-Smith and Kulikowski, 1975). Accordingly, the estimated bandwidth of the theoretical LSF can vary considerably, being much narrower in the latter case.

King-Smith and Kulikowski (1975) were the first to show that the space-domain characteristics of the LSF also depend on temporal aspects of the stimulus. The LSFs obtained with transient stimulation are much broader than those obtained with sustained stimuli. This result was subsequently confirmed and interpreted in terms of spatial characteristics of specific transient (Y) and sustained (X) mechanisms (Wilson, 1978a, b; Wilson and Bergen, 1979).

According to recent computational theories, directional sensitive units consist in pairs (Watson and Ahumada, 1983; van Santen and Sperling, 1984), or triplets (Marr and Ullman, 1981) of adjacent spatial frequency selective receptive fields. The larger the separation between these constituent receptive fields, the more elongated along the direction of drift is the motion receptive field. The area differences between constituent (supposedly subserving detection) and composite (supposedly subserving direction selectivity) receptive fields should be reflected in their respective spatial integration characteristics. Recent psychophysical studies do provide some indirect evidence for such anisotropic, direction sensitive receptive fields (Nakayama *et al.*, 1982; Nakayama and Silverman, 1985; Nakayama, 1985).

This study was intended to provide a direct comparison between the spatial integration characteristics of the detection and direction identification processes. Detection and identification thresholds were concomitantly measured for drifting sinusoidal gratings of various spatial and temporal frequencies. The thresholds were measured as a function of stimulus width (at a constant height), of stimulus height (at a constant width) and of stimulus area (with both width and height varied simultaneously). The empirical width/sensitivity detection and identification functions were fitted with predictions of Wilson and Bergen's (1979) and van Santen and Sperling's (1984) models, respectively. These models have been extensively tested previously and produced rather satisfying fits of empirical data obtained under a large range of experimental conditions. Moreover, their analytical formulation is such that it can be

easily approximated through numerical computation. Still, other detection and direction-identification models might be tested against the empirical size/sensitivity functions. Watson and Ahumada's (1983) motion sensor might be such a candidate because of its linear behaviour. As will be discussed below, the linearity of the motion device may be critical in producing size/sensitivity functions compatible with the detection ones.

## METHODS AND PROCEDURE

### *Stimuli*

All stimuli were patches of vertical sinusoidal gratings of spatial frequency,  $f$ , drifting leftward or rightward with a temporal frequency  $\omega$ ; their luminance ( $L$ ) profile in space ( $x$ ) and time ( $t$ ) can thus be specified by

$$L(x, t) = L_0[1 + m \cos(2\pi f x \pm 2\pi \omega t)] \quad (1)$$

where  $L_0$  is the mean luminance and  $m$  is the depth of modulation. All stimuli were spatially confined by either a rectangular or circular window, depending on the experimental condition. The rectangular windows were fixed either in height or in length at a constant size equal to two periods of the grating stimulus. The variable side of the rectangle could be as small as an eighth of a cycle and as large as 8 cycles. The same range of variation was applied to the radius of the circular window. Three spatial (0.5, 1 and 4 cycles/deg) and three temporal (1, 8 and 16 Hz) frequencies were examined. For the 0.5 and 4 cycles/deg stimuli all three temporal frequencies were studied, but only the 16 Hz modulation was used with the 1 cycles/deg stimulus. These combinations allowed the examination of spatial integration characteristics for five different velocities two of which were common to different spatio-temporal stimuli.

The stimuli were generated by a Picasso CRT Image Generator under computer control (M/OS-80 Mostek microsystem) and were displayed on the face of a Tektronix 608 monitor (P4 white phosphor) at a mean luminance of 88 cd/m<sup>2</sup>. The inspection field was surrounded by a large (100 × 80 cm) white surface of about equal brightness.

In order to obtain the largest range of window sizes the viewing distance was varied from 57 to 230 cm. Within this range the largest aperture used with 0.5 cycles/deg stimuli could not exceed 4 cycles, whereas the smallest one for the 4 cycles/deg stimuli was limited to 0.25 cycles. Fixation was facilitated by means of four tiny black dots 1 cm apart. All stimuli were viewed binocularly with natural pupils by the author. A partial replication of the experiment was obtained with a second observer. Both observers had normal vision.

### *Procedure*

Thresholds were measured by means of a 2 × 2 alternative forced choice (AFC) staircase procedure. The stimulus appeared in one of two 1-s temporal intervals marked by four tones. It could be either a leftward or a rightward drifting grating. The observer had to decide which of the two intervals contained the stimulus (*detection* response) and what was its drift direction (*identification* response). Auditory feedback was provided for both incorrect detection and identification responses. Depending on the experimental session, the staircase increment and decrement rules were made detection or identification dependent. The contrast fed into the computer at the beginning of each staircase was the corresponding threshold as previously estimated by an adjustment procedure.

Three consecutive correct (detection or identification) responses resulted in a 2 dB decrease in contrast, whereas one incorrect response resulted in an identical increase. This produces a detection (or identification) level of 79.6% on the psychometric function (Wetherhill and Levitt, 1965).

In most of the cases where the identification performance was sufficiently close (overall percentage-correct higher than 70%) to the detection performance, only detection dependent rules were used. In these cases the identification threshold could not be directly estimated from the contrast reversals produced by the staircase. This is one of the reasons why the contrast threshold for the two tasks was always estimated at the end of each experimental session by fitting a psychometric function to the raw data. This was done in the following way. The contrasts used by the staircase procedure were stored in the computer memory together with their corresponding percentages of correct responses for both detection and identification responses. Given that sensitivity was independent of drift direction these percentages were calculated from the cumulated responses to the leftward and rightward moving stimuli. This procedure generated at least three (but frequently four or five) frequency of seeing datum points computed from at least 30 repetitions per contrast level. In order to attain this criterion one experimental session consisted of at least 200 (but frequently more than 400) trials distributed in two or three blocks. The fitted psychometric function was of the type proposed by Quick (1974), where the probability of seeing,  $P_i$ , is given by

$$P_i = 1 - (1 - \gamma) \exp [ - (c_i/\alpha)^\beta ] \quad (2)$$

with  $\gamma$  the correction for guessing (0.5 in this case),  $c_i$  the contrast of the stimulus,  $\beta$  the slope of the psychometric function and  $\alpha$  the detection threshold (as it will be displayed in all the following figures) at 81.6% correct. The fitting procedure was a version of that described by Watson (1979), where the maximum likelihood ratio of the theoretical binomial distribution of the observed correct responses was searched for all possible combinations of  $\alpha$  and  $\beta$  within a two octaves range.

The experimental procedure produces thus two threshold estimates, one which is the average contrast of all the contrast reversals within one staircase and a second which is the  $\alpha$  of the Quick psychometric function. For a given spatial and temporal frequency the threshold estimates at different window sizes were obtained in a random order. In most of the cases a complete area/sensitivity function was obtained in two consecutive days. The three temporal frequencies were also randomized while the spatial frequency was kept constant. Many datum points were remeasured at intervals as long as one month to check for observer's reliability over time.

## RESULTS

One reason why the observer's sensitivity was estimated from the  $\alpha$ -parameter of the psychometric function was that comparisons of detection and identification performances cannot be made unless the slopes ( $\beta$ ) of their respective psychometric functions are assumed to be identical. Figure 1 shows distributions of  $\beta$ -estimates as obtained from the 111 detection and 107 identification psychometric functions. The estimated  $\beta$  values did not show any systematic variability with either spatial or temporal frequency, or stimulus size. As can be seen, the two  $\beta$ -distributions are mostly overlapping with the identification  $\beta$ -distribution being significantly broader than the detection one:  $\beta$ -detec. =  $3.12 \pm 0.079$ ;  $\beta$ -identif. =  $3.4 \pm 1.2$ . Assuming that the psychometric function is a cumulative Gaussian and that Quick's (1974) formula roughly

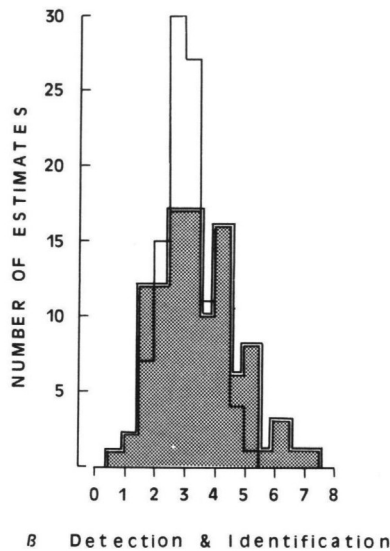


Figure 1.  $\beta$ -detection and  $\beta$ -identification histograms (white and grey areas, respectively. Observer A.G.)

approximates it, it can be shown that average detection and identification  $\beta$  values correspond to standard deviations of approximately 37% and 33%, respectively (e.g. Luce, 1963).

The larger variance of the identification distribution is probably due to a bias in the estimation of  $\beta$ , rather than to the intrinsic variability of the identification process. Since, as mentioned above, the identification psychometric functions were estimated in many cases from detection-dependent staircases, they were typically based on percentages within the lower range of the function. Simulations performed in our laboratory by R. Humbert and K. O'Regan with the likelihood ratio fitting procedure show that  $\beta$ -distributions are typically broader when estimated from data points covering a limited rather than the complete range of the psychometric function (see also Levitt, 1971).  $\alpha$ - and  $\beta$ -means are, nevertheless, rather insensitive to these manipulations. Given these considerations, it can be concluded that the detection and identification thresholds can be reliably compared.

#### *Variable 'number of bars' experiments*

Figures 2 and 3 display detection (solid symbols) and direction identification (open symbols) thresholds for 0.5, 1 and 4 cycles/deg stimuli, respectively, as functions of their width (expressed in number of cycles). The length of the bars was kept constant at 2 cycles. Temporal frequency is given as a parameter. Circles and squares are for observers A.G. and V.T., respectively.

The overall shape of the width/sensitivity curves seems to depend mostly on the spatial frequency of the stimuli: both detection and identification thresholds decrease more rapidly with increasing size for high than for low spatial frequencies. At a given spatial frequency, the shape of these curves does not seem to vary with temporal frequency and appears therefore to be velocity-independent. This can be seen when comparing width/sensitivity functions obtained at equal velocities (e.g. 2 deg/s: 0.5 cycles/deg—1 Hz, Fig. 2, and 4 cycles/deg—8 Hz, Fig. 3).

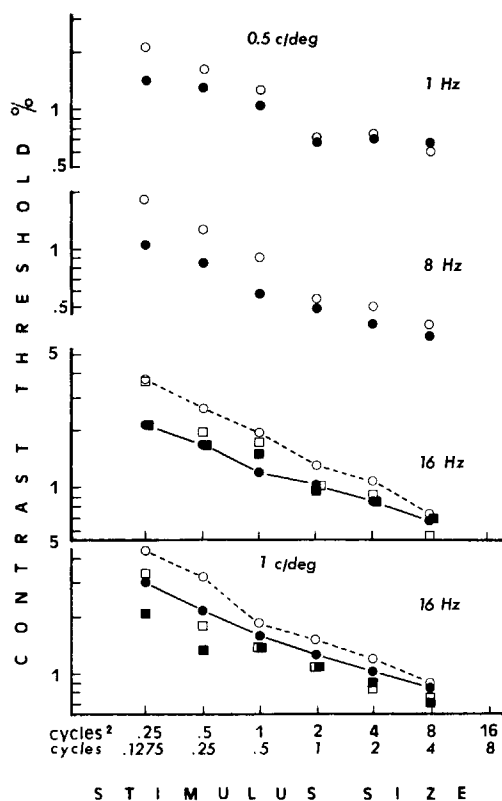


**Figure 2.** Detection (solid symbols) and direction-identification (open symbols) thresholds as a function of stimulus width at a constant length of 2 cycles. The abscissa displays both the width and the corresponding area of the stimulus. Results for the 0.5 and 1 cycles/deg stimuli are displayed in the upper and lower panel, respectively. Temporal frequency is given as a parameter. Circles and squares refer to observers A.G. and V.T., respectively.

Identification thresholds converge and equal the detection thresholds for sizes ranging between 0.5 and 1 period of width. This is so whatever the temporal or spatial frequency of the stimulus. Moreover, direction identification thresholds could be reliably measured for sizes as small as an eighth of a cycle! Even for these extreme conditions the detection-to-identification sensitivity ratio never exceeded a factor of 1.9. For stimuli displaying more than 2 cycles, ratios of 1 were found even within that spatio-temporal range where subthreshold summation experiments did not show complete independence between directional sensitive mechanisms [conditions 4 cycles/deg—1 Hz and 4 cycles/deg—16 Hz are out of the independence range as measured by Watson *et al.* (1980) and Gorea and Lorenceau (1984)]. It should be finally noted that the identification curves may be looked on as horizontal translations of the detection ones. Rather good fits of the identification curves can be obtained by displacing the detection curves toward widths larger by a factor of about 1.5 and 2.0 for low (0.5 and 1 cycles/deg) and high (4 cycles/deg) spatial frequencies, respectively. As will be discussed below this observation cannot be used in a straightforward manner to infer the size of the direction-selective receptive fields, nor does it necessarily imply that these latter are by this much larger than the receptive fields responsible for detection.

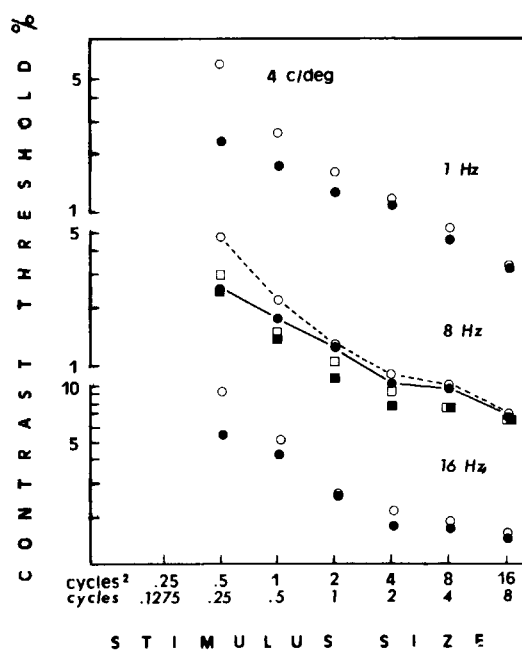


Figure 3. As in Fig. 2 but for a 4 cycles/deg stimulus.

#### *Variable 'lengths of bars' experiments*

The influence of the length of bars on the detection and identification sensitivity was measured only for three experimental conditions. Figure 4 shows these results (right panels) together with the corresponding conditions in the variable 'number of bars' experiments (left panels). Symbols are as in Figs 2 and 3. Note that: (1) for both observers the detection results obtained in the variable length condition are (as displayed) practically the mirror image of the detection results obtained with a variable width; (2) this is not the case for the identification results which appear to be less sensitive to the length of the bars than they are to their number (note, nevertheless, the 4 cycles/deg—8 Hz condition where observer V.T. displays practically confounded detection and identification curves for both variable width and variable length experiments); (3) at the particular width used in the variable length experiment (i.e. 2 cycles) the identification length/sensitivity curves appear to be shifted upward with respect to the detection curves by a constant factor of about 1.2 and 1.1 for observers A.G. and V.T., respectively. This implies that directional selective mechanisms are somehow less sensitive than detection mechanisms, but that they have equal spatial bandwidths along the axis orthogonal to the direction of drift.

An ANOVA performed on the derived detection-to-identification threshold ratios obtained for this particular set of data confirms this description of the results. It shows a strong effect of the size factor in the variable widths experiments ( $F_{5,5} = 42.1$ ,  $P < 0.0005$ ) with no significant effect in the variable length experiments ( $F_{5,5} = 5.01$ ,  $P > 0.05$ ). The spatio-temporal characteristics of the stimulus do not have any significant effect on the detection-to-identification ratios obtained in either the variable width, or the variable length experiments.



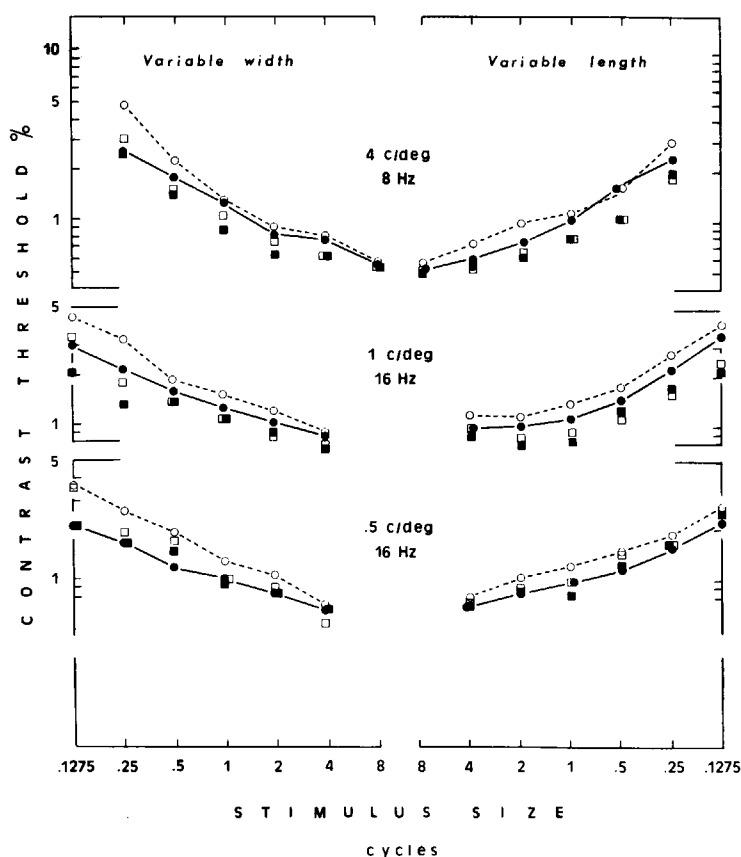


**Figure 4.** 'Variable width' and 'variable length' experiments compared. The 'variable length' data were obtained for a constant width of 2 cycles. The 'variable width' data are from Figs. 1 and 2. Note that the 'variable length' datum points are displayed on a reversed abscissa. Spatial and temporal frequency are given as parameters. Open and solid symbols refer to identification and detection thresholds. Circles and squares are for observers A.G. and V.T., respectively. Solid and dashed lines are drawn for observer A.G.

#### 'Circular aperture' experiments

Had the detection receptive field been non-oriented and isotropic, the detection *area/sensitivity* curves measured with either a constant bar length, or a constant number of bars, should coincide with the detection *area/sensitivity* curves measured for stimuli with both length and width variable. This should be so to the extent that the spatial integration process is linear. On the other hand, this should not be the case for the identification thresholds which show width/length asymmetries. Figure 5 shows detection and identification thresholds obtained with a circular aperture of variable radius (solid and open stars, respectively) together with the results already displayed in Fig. 4 (detection and identification, solid and open symbols, respectively; variable width and length, circles and squares, respectively).<sup>3</sup> Note that the abscissa is given in squared cycles.

The 'variable radius' experiment shows that direction of drift performances can be reliably measured for stimulus areas as small as 0.01227 squared cycles! Even for such small grating patches the detection-to-identification sensitivity ratio does not exceed a

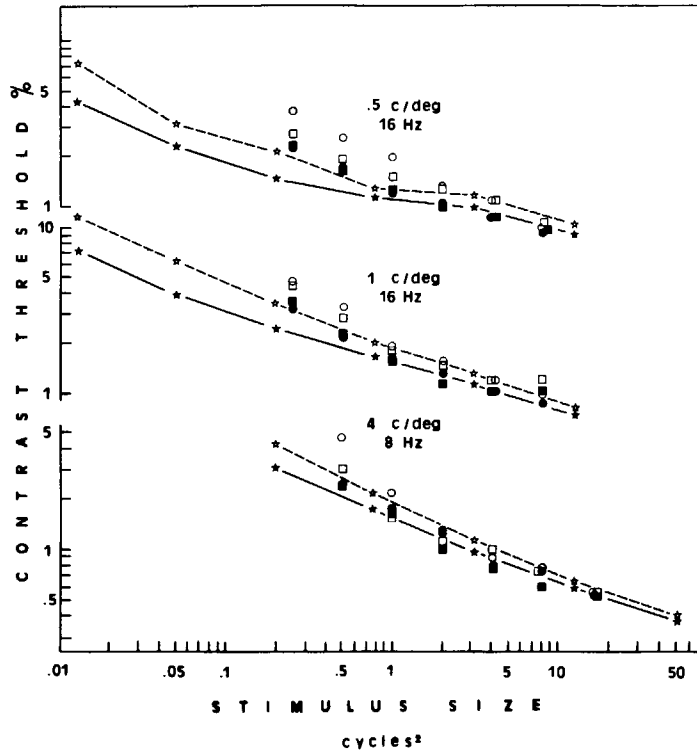


**Figure 5.** Detection (solid symbols) and identification (open symbols) thresholds obtained in the 'variable width' (circles) and the 'variable length' (squares) experiments compared to thresholds obtained in the 'variable radius' experiment (stars). The abscissa represents stimulus area. Observer A.G.

1.7 factor. Comparison of the three experiments clearly indicates that the expected coincidence of the detection area/sensitivity curves does not hold. The three sets of curves converge for stimulus sizes approximately equal to one squared cycle, but the 'variable radius' detection thresholds are always lower for areas below this limit. Spatial integration appears thus to be more effective when one of the stimulus spatial dimensions (width or length) is kept constant than when both dimensions are simultaneously increased. Given the similarity of the 'variable width' and 'variable length' detection results (see Fig. 3), this discrepancy is more likely to be due to some basic nonlinearity in the two-dimensional spatial integration process rather than to an anisotropy of the detection receptive fields. However, the nature of such a nonlinearity will not be discussed here and the following sections will deal only with the integration characteristics along one single spatial dimension.

#### THEORY AND DISCUSSION

To the question concerning the minimum spatial extent of a spatially periodic drifting stimulus below which the direction of drift cannot be perceived anymore, a typical *ad hoc* answer would be 'half a cycle'. These experiments demonstrate that this answer is wrong and that, all in all, the detection and direction-identification spatial integration functions are surprisingly similar. The main results can be summarized as follows. (1) The spatial integration characteristics of both detection and direction-identification

processes are spatial frequency but not temporal frequency dependent. Consequently, they are also velocity independent. (2) Direction identification thresholds can be reliably measured for grating patches with widths as small as 0.1275 cycles (or 0.012 cycles<sup>2</sup> in the circular aperture experiments). Even for these extreme conditions the detection-to-identification sensitivity ratio does not exceed a factor of 2. (3) Detection and identification performances converge and become equal for stimulus sizes greater than, or equal to 0.5 or 1 (depending on the observer) cycles of width. (4) The two-dimensional spatial integration characteristics are isotropic for the detection but not for the identification process. (5) Detection and identification performances as a function of stimulus area are not directly predictable on the basis of the integration characteristics along one spatial dimension. What should be the one dimensional properties of the underlying detection and direction-identification receptive fields accounting for these results?

The measure of the size/sensitivity functions can be directly used to answer this question. This is not the case in experiments dealing with the 'short-range motion process' (Braddick, 1974, 1980) where the critical size is more readily expressed in terms of the physical dimensions of the stimuli rather than of the underlying mechanisms. Moreover, the use of spatially periodic but confined stimuli obviates the debate concerning the relevant parameters that should be used to quantify these physical limits as they can be assessed through variations in the spatio-temporal characteristics of random dot kinematograms (e.g. Baker and Braddick, 1982a, b; Lapin and Bell, 1976; Petersik *et al.*, 1983).

#### *Detection receptive fields*

Robson and Graham (1981) and more recently Tyler and Mayer (1984) used a simplified probability summation model to fit size/sensitivity functions obtained with grating patches extending beyond the limits of linear integration. Since the spatial sensitivity profile of the underlying mechanisms is irrelevant in predicting sensitivity variations exclusively due to spatial probability summation, their model did not include such sensitivity weighting functions. A more elaborate model was provided by Legge (1978) who inferred the line spread function (LSF) of the 'most sensitive mechanism' from empirical size/sensitivity curves. His approach was nevertheless incomplete to the extent that it disregarded parameters such as the drop in sensitivity with eccentricity, probability summation among spatially (and frequency) tuned mechanisms and variations of the LSF with the temporal characteristics of the stimulus.

All these parameters were included in Wilson and Bergen's (1979) model postulating the existence of four spatial and two temporal frequency channels. While the required number of spatial frequency channels has been subsequently set to six (Wilson *et al.*, 1983; Wilson and Gelb, 1984), or to at least seven (Watson, 1982), it is shown below that the initial model provides sufficiently accurate predictions of the data obtained in the present study. The model, whose mathematical description is given in equation (3), includes a basic nonlinearity interpreted in terms of probability summation [according to Quick's (1974) formulation, where  $\beta$  is the slope of the psychometric function] across space,  $x$ , and channels,  $i$

$$R = \left\{ \sum_{i=1}^4 \int_{x-4^\circ}^{x+4^\circ} dx \left[ \int_{-\infty}^{\infty} L(x') LSF_i(x, x') dx' \right]^\beta \right\}^{1/\beta} \quad (3)$$

with  $L(x')$  the luminance profile of the stimulus and  $LSF_i(x, x')$  the line spread function of unit  $i$  centred at eccentricity  $x$ .

Only minor modifications are needed in order to use this model to predict size/sensitivity functions. Parameters showing interobserver variability (see Table 1 in Wilson and Bergen, 1979) were averaged and used as such in the computations. The  $\beta$  exponent was set at 3.4 (see Results and Fig. 1).

Predictions of the model can be obtained by using either transient- or sustained-type parameters, depending on the temporal characteristics of the stimulus. The use of one single type of transient parameters to fit the data of this study is reasonable given the invariance of the size/sensitivity curves with temporal frequency. The width of the stimulus determined the limits of the integration in equation (3).

Note that the stimuli used in the present experiments were drifting gratings of the form given by equation (1). Using this equation as an expression of  $L(x')$  in equation (3) would require a supplementary convolution in the time domain and will substantially complicate its numerical evaluation. A compromise solution was adopted. Equation 3 was independently evaluated for  $L(x')$  in sine and cosine phases. The outcomes were summed probabilistically in line with the idea of probability summation over time (Watson, 1979; Gorea and Tyler, 1985) and with the space-time separability hypothesis (Kelly, 1962; Watson and Nachmias, 1977; Wilson, 1980). Introduction of more than two phases in the numerical evaluation of equation (3) had practically no effect on the overall shape of the predicted size/sensitivity function.

Given the shape invariance of the size/sensitivity functions with temporal frequency, the contrast thresholds measured for each spatial frequency were geometrically averaged across temporal frequency. They are shown in Fig. 6 together with the final outcome of the simulations (continuous curves; the dashed curves are discussed

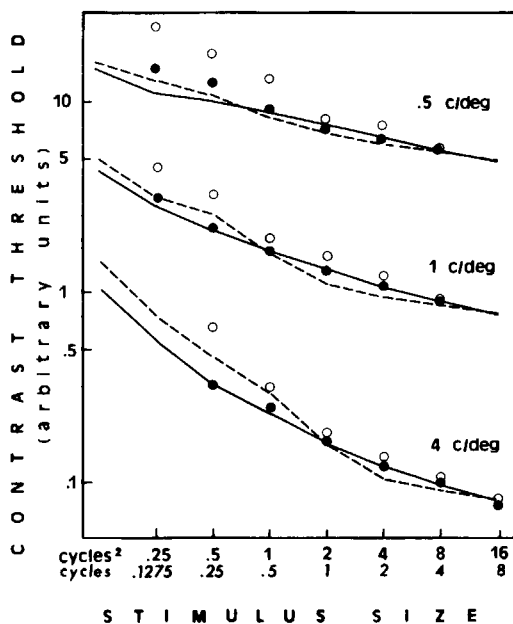


Figure 6. Detection (solid symbols) and identification (open symbols) thresholds averaged across temporal frequency and predictions of Wilson and Bergen's (1979) and van Santen and Sperling's (1984) models (solid and dashed curves, respectively. See text for details.)

below).<sup>4</sup> While the absolute predicted threshold values depend on a temporal frequency sensitivity parameter which was arbitrarily set to one, the shapes of the measured and predicted size/sensitivity functions are in good agreement. Slight deviations for the small apertures with the 0.5 cycles/deg gratings might be due both to the computational approximation of the spatio-temporal convolution and to the existence of additional spatial mechanisms more sensitive within this spatial frequency range. Note that, in agreement with the data, the simulated functions become steeper as spatial frequency is increased. Consequently, when expressed in periods of the stimulus, the space constant of the integration process as obtained from the intersection of its two limiting asymptotes [i.e. of slopes  $-1$  and  $-1/\beta$  in the pure integration and in the pure probability summation spatial ranges—see Gorea and Tyler (1985) for a discussion of this point] decreases with spatial frequency.

#### *Direction-identification receptive fields*

Size/sensitivity functions for the identification process can be approximately fitted by linearly translating the detection curves toward sizes larger by a factor of about 1.5–2. This suggests the existence of direction sensitive receptive fields similar to the detection ones but with a larger spatial spread. Nevertheless, the outcome of the spatial integration simulations obtained for each of the four mechanisms proposed by Wilson and Bergen indicates that an increase in the receptive field size does not necessarily generate the required shape of the spatial integration function to fit the identification data.<sup>4</sup>

Before trying to generate more appropriate receptive field profiles let me discuss the following. Variations in the spatial aperture of the drifting stimulus produce inversely related variations in its spatial (but not temporal) frequency content. Since in the present experiments the temporal presentation window was kept constant, the spread in the spatial frequency spectrum was correlative of a proportional spread in the velocity spectrum of the stimulus. If a drifting stimulus of spatial frequency  $f$  is windowed to a spatial extent narrower than half of its spatial period, the corresponding spatial frequency spread will extend beyond the origin of the spatial frequency axis. Consequently, the spectrum of the spatio-temporal stimulus will include opposite directions of motion. [(This aperture problem is nicely illustrated and generalized by Watson and Ahumada (1985)).

Deciding on the global direction of motion of such a complex stimulus will therefore become an ambiguous task, *independently of the actual sensitivity profiles of the underlying receptive fields*. The exact relationship between this physical ambiguity and the measured direction-identification performances remains to be assessed. It will obviously depend not only on the relative energy contained in the even and odd quadrants of the spatio-temporal frequency plane and on the sensitivity characteristics of the visual system, but also on some unknown decision rules of the observer. If the divergence of the detection and direction-identification thresholds for spatial apertures smaller than half a period of the stimulus could be accounted for in terms of this physical ambiguity, the underlying direction-sensitive receptive fields would be indistinguishable from the detection receptive fields. Had this physical ambiguity played a limited role in the identification performances, only minor sensitivity profile differences would be required to account for the direction-identification functions.

Still, recent models of visual motion perception propose that directional information is processed from the combined output of at least two adjacent, detection-type

receptive fields (Marr and Ullman, 1981; Watson and Ahumada, 1983, 1985; van Santen and Sperling, 1984, 1985; Adelson and Bergen, 1985). Pairs of symmetric or symmetric-antisymmetric receptive fields might account as well for directional sensitivity. Obviously, the coupled receptive fields predictions will depend on such parameters as the type of coupling (symmetric-symmetric vs symmetric-antisymmetric), the distance between the coupled receptive fields and the type of computation required to achieve directional selectivity. Van Santen and Sperling's (1984) original Reichardt-type model was chosen here to simulate size/sensitivity functions because of its computational simplicity. Indeed, if the first level temporal and spatial filters are chosen such that they display optimal time and phase shifts (e.g. Nakayama and Silverman, 1985) Van Santen and Sperling's (1984) model [see their equation (15)] reduces to

$$R = m^2 ds R_{\text{left}}, R_{\text{right}} \quad (4)$$

where  $m$  is the stimulus modulation;  $d$ , its direction of drift (i.e.  $-1, 0, 1$ );  $s$ , a sensitivity parameter; and  $R_{\text{left}}, R_{\text{right}}$ , the responses of the two adjacent receptive fields after spatial convolution with the stimulus.

In order to provide direct comparisons with the detection size/sensitivity functions (Fig. 6), the spatial outputs  $R_{\text{left}}$  and  $R_{\text{right}}$  in equation (4) were computed through convolution of the stimulus with the receptive field profiles described by Wilson and Bergen (1979). The outputs of the four types of symmetric-symmetric receptive field pairs were simultaneously computed for sine and cosine spatial phases. The sensitivity parameter was arbitrarily set to one. The final output of the system was obtained through probability summation across space, mechanisms and phases. As for the detection simulations, the probability summation exponent was set to 3.4. The outcome of the simulations are displayed as dashed curves in Fig. 6 for the three studied spatial frequencies. If vertically shifted such as to equate the detection and identification thresholds for the largest sizes, the two sets of functions slightly diverge at smaller apertures with a maximum detection-to-identification ratio of about 1.5 for the 4 cycles/deg stimulus. If the detection and identification functions were directly comparable, it could have been suggested that the identification performances are only partly limited by the shape of the underlying receptive fields with additional limitations due to the spread of the velocity spectrum as discussed above. Nevertheless, because of differences in the overall shape of the size/sensitivity functions for individual and coupled receptive fields, no such conclusion can be drawn.

Comparison of the detection and identification size/sensitivity functions as displayed in Fig. 6 reveals the shallower threshold decrease produced by the coupled receptive fields at large spatial apertures. This is due to the nature of the detection and identification models used in the present simulations. While in equation (3) stimulus modulation  $m$  intervenes as such, it is squared in equation (4) because of the multiplicative interaction between the coupled receptive fields in van Santen and Sperling's nonlinear model. It can be easily shown that, had sensitivity been constant across eccentricity, the decrease in the contrast threshold for stimulus sizes beyond the linear integration area would be asymptotic to a slope of  $-1/\beta$  and  $-1/2\beta$  for the detection and direction-identification models, respectively (see Watson, 1979; Gorea and Tyler, 1985). If detection and identification size/sensitivity functions are equated such that they coincide for the largest apertures, they will cross each other at smaller apertures with identification performances being better than detection performances

within this size range. Such a possibility can be excluded on both logical and empirical grounds. This leads to an important observation: detection and identification units, if different, *must* operate according to the *same*, linear or nonlinear, characteristics. More specifically, injecting stronger nonlinearities in the motion than in the detecting sensor, will produce an atypical behaviour of the detection-to-identification ratio as a function of stimulus size (or duration).

In a recent and elegant paper Adelson and Bergen (1985) discuss the differences and similarities of two general classes of models accounting for direction sensitivity, i.e. energy- and Reichardt-type models. In their final chart (see their appendix and Fig. 18) they show that the two models are equivalent, except for a scale factor. This is nevertheless true provided that the energy models are required to be *phase insensitive*. This property is achieved through a squaring operation on the outputs of the two individual, first-level input units. The squaring operation provides these models with the same nonlinearity as the Reichardt-type ones. Consequently, both energy and Reichardt models will produce the same 'anomalous' spatial (or temporal) integration functions relative to the spatial (or temporal) characteristics of the detection units. There are at least three possibilities to avoid this incongruity. One is to let the energy-type motion unit be phase sensitive and to take advantage of this property in velocity computation (Watson and Ahumada, 1985). A second alternative is to achieve phase independency through rectification by an 'absolute', rather than by a squaring operator. This alternative has been proposed by Watson (1979) to account for temporal integration characteristics and more recently discussed by Gorea and Tyler (1985).

Finally, the third solution is contingent upon a preliminary question which remains to be answered. Is there sufficient empirical and theoretical evidence to show that detection of a drifting stimulus is prior to and/or takes place at a different decision level than direction identification? The size/sensitivity functions measured in the present experiments do not provide a clearcut answer to this question. The divergence of the detection and identification functions when stimulus size is reduced is sufficiently small to be attributed to the spread of the velocity spectrum rather than to significant size differences between motion and detection receptive fields. It therefore remains that the existence of directionally labelled *detectors* is still plausible. This implies that directional sensitivity is achieved at the detection threshold and that detection and direction-identification processes cannot therefore be discriminated. Had this been the case, it would still be needed to find out whether this unique output reflects the activity within single or coupled spatial frequency selective receptive fields.

### Acknowledgements

This work was supported by a CNRS research grant, ATP No. 955130. I am grateful to Ken Nakayama and Kevin O'Regan for their comments on an earlier version of this paper.

### REFERENCES

- Adelson, E. H. and Bergen, J. R. (1985). Spatiotemporal energy models for the perception of motion. *J. Opt. Soc. Am.* **A2**, 284–299.
- Aubert, H. (1865). *Physiologie der Netzhaut*. Morgenstern, Breslau.
- Ball, K., Sekuler, R. and Machamer, J. (1983). Detection and identification of moving targets. *Vision Res.* **23**, 229–238.
- Baker, C. L. Jr and Braddick, O. J. (1982a). Does segregation of differently moving areas depend on relative or absolute displacement? *Vision Res.* **22**, 851–856.

- Baker, C. L. Jr and Braddick, O. J. (1982b). The basis of area and dot number effects in random dot motion perception. *Vision Res.* **22**, 1253–1259.
- Bartlett, N. R. (1965). Thresholds as dependent on some energy relations and characteristics of the subject. In: *Vision and Visual Perception*. C. H. Graham (Ed.). John Wiley, New York (pp. 154–184).
- Bergen, J. R., Wilson, H. R., and Cowan, J. D. (1979). Further evidence for four mechanisms mediating vision at threshold: sensitivities to complex gratings and aperiodic stimuli. *J. Opt. Soc. Am.* **69**, 1580–1587.
- Braddick, O. J. (1974). A short-range process in apparent motion. *Vision Res.* **14**, 519–527.
- Braddick, O. J. (1980). Low-level and high-level processes in apparent motion. *Phil. Trans. R. Soc. Lond.* **290B**, 137–151.
- Campbell, F. W. and Robson, J. G. (1968). Application of Fourier analysis to the visibility of gratings. *J. Physiol., Lond.* **197**, 551–566.
- Daugman, J. G. (1980). Two-dimensional spectral analysis of cortical receptive fields profiles. *Vision Res.* **20**, 837–846.
- Fiorentini, A. (1971). Excitatory and inhibitory interactions in the human eye. In: *Visual Sciences: Proceedings of the 1968 International Symposium*. J. R. Pierce and J. R. Levine (Eds). Indiana University Press, Bloomington, Indiana (pp. 269–283).
- Gorea, A. (1984). Spatial and temporal characteristics for two types of detection/identification tasks. *J. Opt. Soc. Am.* **74A**.
- Gorea, A. and Lorenceau, J. (1984). Perceptual bistability with counterphase gratings. *Vision Res.* **24**, 1321–1331.
- Gorea, A. and Tyler, C. W. (1985). A new look at Bloch's Law for contrast. *J. Opt. Soc. Am.* (in press).
- Graham, N. (1977). Visual detection of aperiodic spatial stimuli by probability summation among narrowband channels. *Vision Res.* **17**, 637–652.
- Green, M. (1983). Contrast detection and direction discrimination of drifting gratings. *Vision Res.* **23**, 281–289.
- Hines, M. (1976). Line spread function variation near the fovea. *Vision Res.* **16**, 567–572.
- Hoekstra, J., van der Groot, D. P. J., van den Brink, G. and Bilsen, F. A. (1974). The influence of the number of cycles upon the visual contrast threshold for spatial sine-wave patterns. *Vision Res.* **14**, 365–368.
- Howell, E. R. and Hess, R. F. (1978). The functional area for summation to threshold for sinusoidal gratings. *Vision Res.* **18**, 369–374.
- Jamar, J. H. T. and Koenderink, J. J. (1983). Sine-wave gratings: scale invariance and spatial integration at suprathreshold contrast. *Vision Res.* **23**, 805–810.
- Kelly, D. H. (1962). New stimuli in vision. In: *Abbiden and Sehen*. H. Schober and R. Rohler (Eds). Straub, Munich (pp. 119–126).
- Kelly, D. H. (1979). Motion and vision. II. Stabilized spatio-temporal threshold surface. *J. Opt. Soc. Am.* **69**, 1340–1349.
- King-Smith, P. E. and Kulikowski, J. J. (1975). Pattern and flicker detection analysed by subthreshold summation. *J. Physiol. Lond.* **249**, 519–548.
- Kulikowski, J. J. (1978). Spatial resolution for the detection of pattern and movement (real and apparent). *Vision Res.* **18**, 237–238.
- Kulikowski, J. J. and King-Smith, P. E. (1973). Spatial arrangement of line, edge and grating detectors revealed by subthreshold summation. *Vision Res.* **13**, 1455–1478.
- Kulikowski, J. J., Bishop, P. O. and Kato, H. (1977). Sustained and transient responses by cat striate cells to stationary flashing light and dark bars. *Brain Res.* **170**, 362–367.
- Lappin, J. S. and Bell, H. H. (1976). The detection of coherence in moving random-dot patterns. *Vision Res.* **16**, 161–168.
- Legge, G. E. (1978). Space domain properties of a spatial frequency channel in human vision. *Vision Res.* **18**, 959–969.
- Levitt, H. (1971). Transformed up-down methods in psychoacoustics. *J. Acoust. Soc. Am.* **49**, 467–477.
- Levinson, E. and Sekuler, R. (1975). The independence of channels in human vision selective for direction of movement. *J. Physiol. Lond.* **250**, 347–366.
- Luce, R. D. (1963). Discrimination. In: *Handbook of Mathematical Psychology*, Vol. I. R. D. Luce, R. R. Bush and E. Galanter (Eds). John Wiley, New York (pp. 191–243).
- Marcelja, S. (1980). Mathematical description of the responses of simple cortical cells. *J. Opt. Soc. Am.* **70**, 1297–1230.
- Marr, D. and Hildreth, E. (1980). Theory of edge detection. *Proc. R. Soc. Lond.* **207B**, 187–217.
- Marr, D. and Ullman, S. (1981). Directional selectivity and its use in early visual processing. *Proc. R. Soc. Lond.* **211B**, 151–180.



- McCann, J. J., Savoy, R. L. and Hall, J. A. Jr (1978). Visibility of low-frequency sine-wave targets: dependence on number of cycles and surround parameters. *Vision Res.* **18**, 891–894.
- Nakayama, K. (1985). Extraction of higher order derivatives of the optical velocity vector field: limitations imposed by the biological hardware. In: *Brain Mechanisms and Spatial Vision*. D. Ingle and M. Jannerod (Eds). Martinus Nijhoff, Dordrecht (in press).
- Nakayama, K. and Silverman, G. H. (1985). Detection and discrimination of sinusoidal grating displacements. *J. Opt. Soc. Am.* **75**, 267–274.
- Nakayama, K., Silverman, G. H., MacLeod, D. I. A. and Mulligan, J. (1985). Sensitivity to shearing and compressive motion in random dots. *Perception* **14** (in press).
- Olzak, L. A. and Thomas, P. (1981). Gratings: why frequency discrimination is sometimes better than detection. *J. Opt. Soc. Am.* **71**, 64–70.
- Pasternak, T. and Merigan, W. H. (1984). Effects of stimulus speed on direction discriminations. *Vision Res.* **24**, 1349–1355.
- Petersik, J. T., Pufahl, R. and Krasnoff, E. (1983). Failure to find an absolute retinal limit of a putative short-range process in apparent motion. *Vision Res.* **23**, 1663–1670.
- Quick, R. F. (1974). A vector magnitude model of contrast detection. *Kybernetik* **16**, 65–67.
- Reichardt, W. (1957). Autokorrelationsauswertung als Funktionsprinzip des Zentralnervensystems. *Z. Naturforsch.* **12B**, 447–457.
- Ricco, A. (1877). Relazione fra il minimo angolo visuale et l'intensità luminosa. *Memorie della Regia Accademia di Scienze, lettere ed arti in modena* **17**, 47–160.
- Robson, J. G. and Graham, N. (1981). Probability summation and regional variation in contrast sensitivity across the visual field. *Vision Res.* **21**, 409–418.
- Savoy, R. L. and McCann, J. J. (1975). Visibility of low-spatial-frequency sine-wave targets: dependence on number of cycles. *J. Opt. Soc. Am.* **65**, 343–350.
- Shade, O. H. (1956). Optical and photoelectric analog of the eye. *J. Opt. Soc. Am.* **46**, 721–739.
- Thomas, J. P. (1968). Linearity of spatial integration involving inhibitory interactions. *Vision Res.* **8**, 49–60.
- Thomas, J. P. and Gille, J. (1979). Bandwidth of orientation channels in human vision. *J. Opt. Soc. Am.* **69**, 652–660.
- Thomas, J. P., Gille, J. and Barker, R. A. (1982). Simultaneous visual detection and identification. *J. Opt. Soc. Am.* **72**, 1642–1651.
- Tyler, C. W. and Mayer, M. J. (1984). Probability summation over space: predictions from a nonlinear signal-detection approach. *J. Opt. Soc. Am.* **74A**.
- van der Wildt, G. J. and Waarts, R. G. (1983). Contrast detection and its dependence on the presence of edges and lines in the stimulus field. *Vision Res.* **23**, 821–830.
- van Santen, J. P. H. and Sperling, G. (1984). Temporal covariance model of human motion perception. *J. Opt. Soc. Am.* **A1**, 451–473.
- van Santen, J. P. H. and Sperling, G. (1985). Elaborated Reichardt detectors. *J. Opt. Soc. Am.* **A2**, 300–321.
- Watson, A. B. (1979). Probability summation over time. *Vision Res.* **19**, 515–522.
- Watson, A. B. (1982). Summation of grating patches indicates many types of detector at one retinal location. *Vision Res.* **22**, 17–25.
- Watson, A. B. and Ahumada, A. J. Jr (1983). A look at motion in the frequency domain. NASA Technical Memo. 84352 (National Technical Information Service, Springfield, Va.).
- Watson, A. B. and Ahumada, A. J. Jr (1985). Model of human visual-motion sensing. *J. Opt. Soc. Am.* **A2**, 322–341.
- Watson, A. B. and Nachmias, J. (1977). Patterns of temporal interaction in the detection of gratings. *Vision Res.* **17**, 893–902.
- Watson, A. B. and Robson, J. G. (1981). Discrimination at threshold: labelled detectors in human vision. *Vision Res.* **21**, 1115–1122.
- Watson, A. B., Thompson, P. G., Murphy, B. J. and Nachmias, J. (1980). Summation and discrimination of gratings moving in opposite directions. *Vision Res.* **20**, 341–347.
- Westheimer, G. (1965). Spatial interaction in the human retina during scotopic vision. *J. Physiol. Lond.* **181**, 881–894.
- Westheimer, G. (1967). Spatial interaction in human cone vision. *J. Physiol. Lond.* **190**, 139–154.
- Wetherill, G. B. and Levitt, H. (1965). Sequential estimation of points on a psychometric function. *Br. J. Math. Stat. Psychol.* **18**, 1–9.
- Wilson, H. R. (1978a). Quantitative prediction of line spread function measurements: Implications for channel bandwidths. *Vision Res.* **18**, 493–496.

- Wilson, H. R. (1978b). Quantitative characterization of two types of line spread function near the fovea. *Vision Res.* **18**, 971–982.
- Wilson, H. R. (1980). Spatiotemporal characterization of a transient mechanism in the human visual system. *Vision Res.* **20**, 443–452.
- Wilson, H. R. and Bergen, J. R. (1979). A four mechanism model for threshold spatial vision. *Vision Res.* **19**, 19–32.
- Wilson, H. R. and Gelb, D. J. (1984). A modified line-element theory for spatial frequency and width discrimination. *J. Opt. Soc. Am.* **73**, 124–131.
- Wilson, H. R., McFarlane, D. K. and Phillips, G. C. (1983). Spatial-frequency tuning of orientation selective units estimated by oblique masking, *Vision Res.* **23**, 873–882.

## NOTES

1. Within the framework of a temporal covariance model as initially developed by Reichardt (1957), stimuli drifting in opposite directions are fed into independent channels with interacting outputs. It follows that under such assumptions the motion/counterphase sensitivity ratio might not be a relevant measure to infer the spatio-temporal characteristics of a motion sensitive device (van Santen and Sperling, 1984). A ratio of two would then reflect either some 'accidental properties' of the spatial and temporal frequency characteristics of the Reichardt unit, or the 'accidental' sensitivity ratio of distinct flicker and motion detecting mechanisms (see pp. 470–471).

2. The problem concerning the relationship between independent detection and perfect identification can be raised for any physical dimension where 'tuned' mechanisms were shown to exist. This is the case for spatial and temporal frequency 'channels' (Olzak and Thomas, 1981; Watson and Robson, 1981; Thomas *et al.*, 1982; Gorea, 1984), orientation 'channels' (Thomas and Gille, 1979), etc. Although the concept of independence between mechanisms is rather easily dealt with by this literature, the concept of 'labelled detector' is more difficult to account for theoretically. As discussed by Watson and Robson, it implies that identification at threshold is based on the activity of one single detector. While under high threshold assumptions the activation of one single detector is quite frequent at the detection threshold, it remains quite improbable from the standpoint of the signal detection theory.

3. Size/sensitivity functions for the remaining spatio-temporal frequency combinations were also obtained in this experimental condition (observer A.G.). However, in order to preserve clarity of illustration and to facilitate comparison with the preceding experiment only a limited sample of the data is presented.

4. The full set of simulations (i.e. for the four detecting mechanisms and the three spatial frequencies) may be obtained from the author on request.